Using a Numerical Model to Verification of Thermoelastic Analysis of Flat Specimen

Milan Sapieta[1], Peter Sulka[1], Martin Svoboda[2]
[1]Faculty of Mechanical Engineering, Univerzity of Zilina. Unierzitna 1, 010 26 Zilina. Slovak Republic. E-mail: milan.sapieta@fstroj.uniza.sk, peter.sulka@fstroj.uniza.sk
[2]Faculty of Mechanical Engineering of Jan Evangelista Purkyně University in Ústí nad Labem, Na Okraji 1001, Czech Republic. E-mail: svoboda@fvtm.ujep.cz

The paper dealt with experimental measurement of stress distribution on flat specimen with circular hole. The main purpose of this paper is comparison of this measurement with numerical analysis. Experimental measurement was realized on loading machine where loaded specimen was recorded with infrared camera and then measured data was evaluated in specialized software. Numerical analysis were carried out by finite element method (FEM). In both cases was evaluated first invariant of stresses which is sum of principal stresses. It was compared maximal and minimal values, layout and course on horizontal and vertical lines of stresses for all 4 load states.

Keywords: FEM simulation, experimental measurement, thermal effect

1 Introduction

Nowadays, a combination of numerous infrared detectors or thermal sensors with advanced signal processing generates a practical tool for investigating thermal-stress characteristics of materials and structures from the respective surface or part of the space.

Thermoelastic stress analysis has been used by engineers and scientists for more than 50 years to address practical problems. It utilises the principle of sensing the energy released during loading in the elastic domain. Once loading is removed, the body returns to its original position (elasticity) and its original temperature (thermoelasticity) [1].

2 Thermoelasticity and dissipative temperature variation

Thermoelastic stress analysis (TSA) is an experimental contactless method based on measuring the infrared radiation emitted from the component surface exposed to dynamically linear elastic strain (deformation). Kelvin was the first scientist to study the thermoelastic effect, and the basic equations to describe the thermoelastic [2] effect were formulated by Darken and Curry.

The general form of the heat conduction equation for elastic body is derived from the energy conservation equation, and it can be written as follows:

$$\rho c_{\varepsilon}\frac{dT}{dt}-\frac{\partial}{\partial x_j}\left(k\frac{\partial T}{\partial x_j}\right)=\rho r+\sigma_{ij}\frac{\partial \varepsilon_{ij}}{\partial t}-\rho\frac{\partial \psi}{\partial V_k}\frac{dV_k}{dt}+\rho T\frac{\partial^2\psi}{\partial T\partial V_k}\frac{dV_k}{dt}, \quad (1)$$

Equation (1) uses the Einstein summation convention, ρ is the density, $\boldsymbol{c_\varepsilon}$ is the specific heat capacity at constant deformation, $\boldsymbol{T}$ is the absolute temperature, $\boldsymbol{k}$ is the thermal conductivity tensor, $\boldsymbol{\sigma_{ij}}$ and $\boldsymbol{\varepsilon_{ij}}$ are the tensors of stress and strain, $\boldsymbol{\varepsilon_{ij}}$ is the inner heat source per unit of volume and $\boldsymbol{\Psi}$ is Helmholtz free energy that is dependent on $\boldsymbol{k}$ and independent of the internal state variables $\boldsymbol{V_k}$.

Provided that the material elastic properties and constant material coefficients are temperature independent, then it can be derived a 3-dimensional heat conduction equation written as follows:

$$\rho c_{\varepsilon}\dot{T}-k\Delta^2 T=T_0\left(-\frac{E\alpha}{1-2\upsilon}\right)\dot{\varepsilon}_1^e+\alpha_p\sigma_{ij}\dot{\varepsilon}_{ij}^p, \quad (2)$$

The equation for heat conduction will include the creation of the thermoelastic and the thermoplastic heat. Parameter $\boldsymbol{\varepsilon_1^e}$ denotes the first invariant of elastic deformation tensor $\boldsymbol{\varepsilon_{ij}^p}$ is the plastic part of the deformation tensor, α is the coefficient of thermal expansion, E Young's modulus, υ Poisson's ratio and $\mathbf{T_0}$ is the initial temperature [3]. Non-dimensional coefficient $\boldsymbol{\propto_p}$ is the ratio of the total plastic work to plastic work, which is converted to heat. The value $\boldsymbol{\alpha_p \cong 1}$ because of only a small part of the plastic work (obtained energy at cold forming) is used to change the inner properties of the material [4-10]. Therefor the thermoplastic area will be neglected and relationship will be formulated only for thermo-elastic area, which has the following form:

$$\Delta T=\frac{\alpha T_0}{\rho c_p}\Delta\sigma_{ii}, \quad (3)$$

Where $\mathbf{c_p}$ is the specific heat capacity under constant pressure and its relationship with $\mathbf{c_\varepsilon}$ is as follows:

$$c_{\varepsilon}=c_p-\frac{2E\alpha^2 T}{\rho(1-\upsilon)}, \quad (4)$$

3 Thermoelastic measurement

Type specimens used in analysis were chosen flat specimens with a circular hole, from material ST 11 523 with a size of 49 x 111 mm with a hole diameter of ϕ=12mm. The hole was placed in the center of the test specimen. Loading was performed in the form of a cyclic load on the ZWICK testing machine (Fig. 1). A thermoelastic analysis was performed on this specimen, which was then

compared with the FEM analysis performed in the ADINA program.

An emissive spray was applied to the surface of the specimen, which is primarily intended for long-range IR cameras, but for the homogenization of its surface, it has now proved to be the best possible solution. To eliminate the influence of external factors during the measurement, polystyrene boards of thickness of 8 cm was placed from 3-sides around test machine (Fig. 1).

Fig. 1 *Layout of measurement apparatus*

The measurement was performed at a cyclic load of 107 Hz. The sampling frequency was 383 Hz, as the maximum resolution was reached. The software manual for evaluating this experiment recommends that you take at least 4 shots during one load period. Since this condition was not fully met ($383/107 \neq 4$), this measurement was slightly sub-sampled, but ultimately it had not effect on the quality of the results because the recording time was up to 10 seconds. During the experiment, the specimen was cyclically loaded only by tension.

For each load state was recorded 3830 thermograms (10s of measurement records). These thermograms were evaluated according to the theory of thermoleasticity described in theoretical part of this paper. The derived relationship uses the ALTAIR-LI software in which, after fitting the material properties of the specimens, we get distributions of the stress field of the main stresses for all 4 loads states (Fig. 2,3).

Stress fields can observed on these specimens using a dynamic range. As the load increases, the signal-to-noise ratio at the IR detector output increases, which is reflected by a decrease in the number of dark (shaded) areas in the images (and also in image sharpness) with increasing load. The maximum positive voltage values are plotted on the left and right edges of the circular hole. These have a decreasing tendency toward the edge of the sample (Fig. 3). Minimum negative stress values are plotted at the top and bottom of the circular hole. These values, as in the case of positive values, are analogous to the upward and downward pattern of the specimen in the jaws of the loader. Inaccuracies in thermograms (the presence of dark shaded areas or low sharpness of the image) (Fig. 2,3) could be removed either by a longer measurement time by increasing the number of thermograms and then achieving greater precision or by using another filter settings for evaluating results. For measurements, the size of one pixel was small enough, so it would be better to use a larger number of pixels to form the median area.

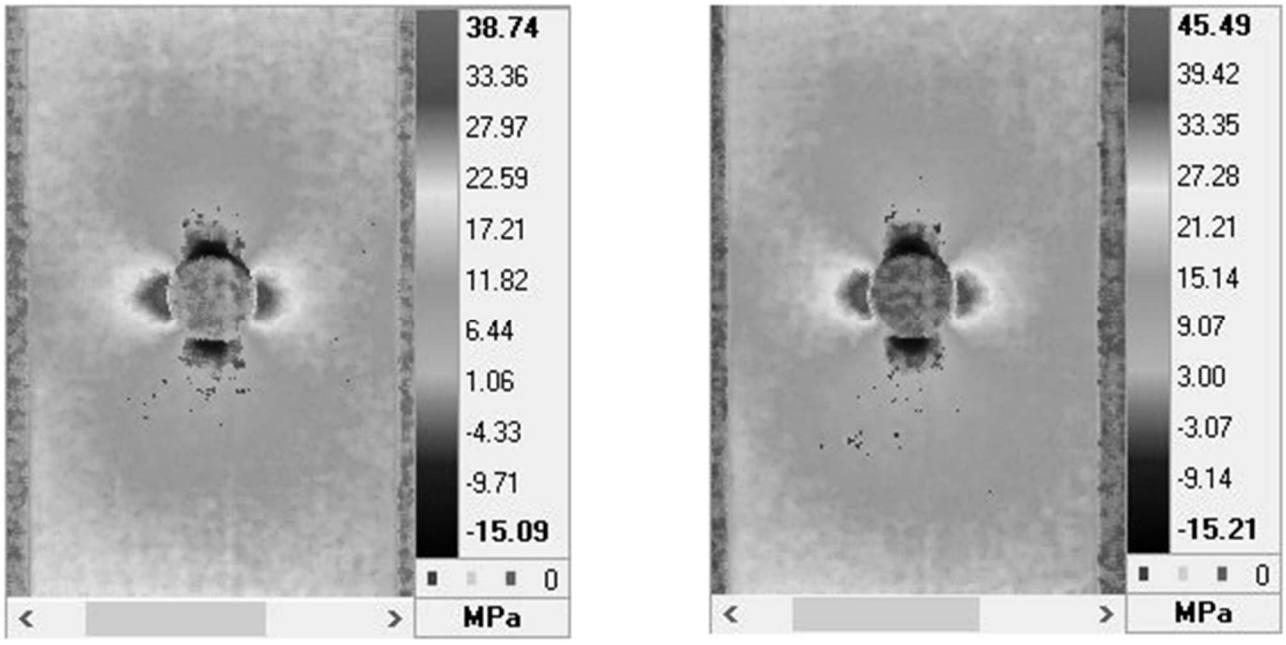

Fig. 2 *Distribution of the main stresses of the flat specimen for a load of 0,6 kN on left side and 0,7 on right side*

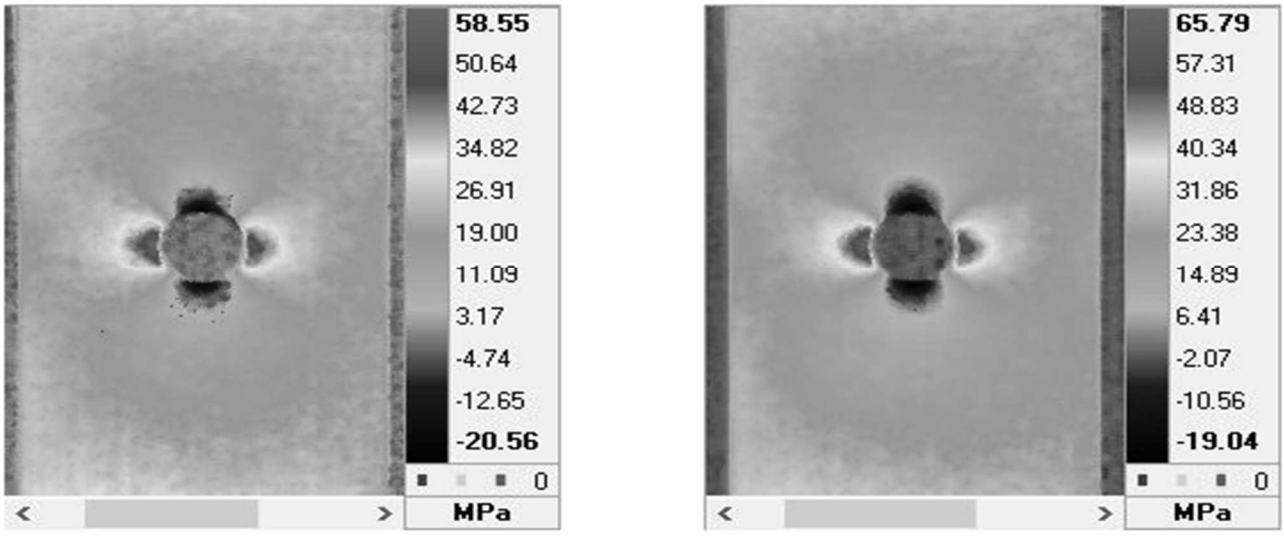

Fig. 3 *Distribution of the main stresses of the flat specimen for a load of 0,9 kN on left side and 1 on right side*

4 The comparison of experiments and numerical solution

The results of FEM analysis are comparable with the results of the experimental measurement. The material properties used were, as opposed to the experimental part, only: Young's modulus of elasticity E = 200GPa and Poisson's μ = 0.3. The geometry of the specimen was identical to the geometry in the experiment with the only difference, that the length was chosen only from the place of attachment in the jaws of the loader. Main stresses were evaluated, as well as in the experimental section. For the maximum stresses in the area of the circular hole are the differences between the FEM analysis and the experimental part in the order of the tenths of MPa, corresponding to a difference of up to 4%. When verifying the minimum stress value, these differences are even greater, mainly due to the poor and unequal stress manifestation of the experimental part. The difference was around 12% on average. Differences are shown in Tab. 1.

Tab. 1 *Comparison of variance of numerical simulation results and experimental measurement*

Load [kN]		Experimental measurement [MPa]	Numerical simulation [MPa]	Derogation in %, [1]
0.6	Min.	-15.09	-14.76	2.23
0.6	Max.	38.74	40.28	3.82
0.7	Min.	-15.21	-17.24	11.77
0.7	Max.	45.49	47.03	3.27
0.9	Min.	-20.56	-22.16	7.22
0.9	Max.	58.55	60.46	3.16
1	Min.	-19.04	-24.61	22.63
1	Max.	65.79	67.14	2.01

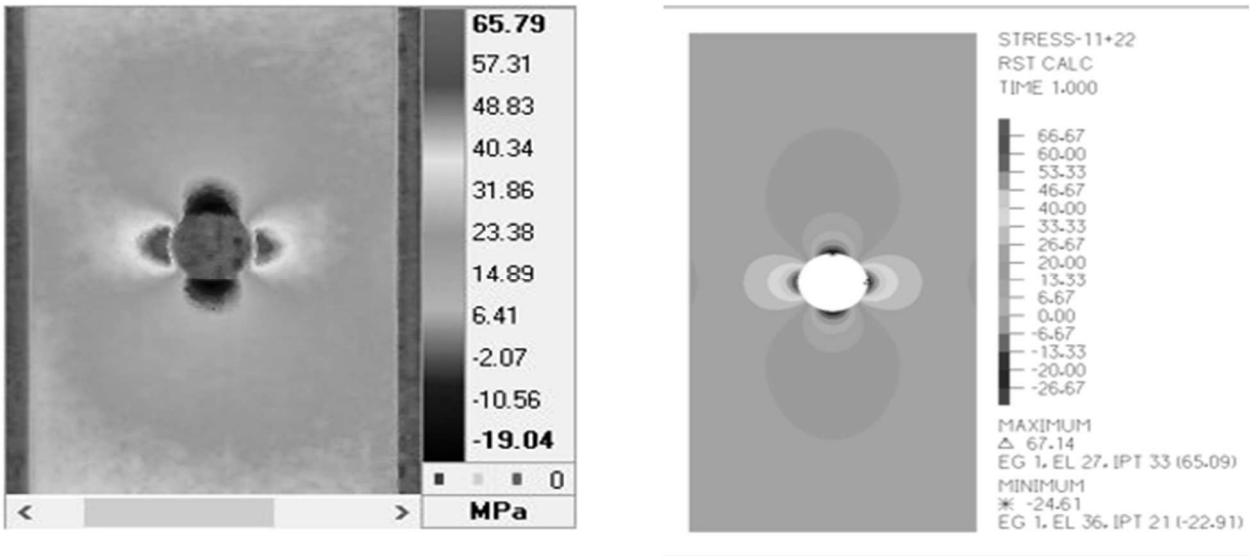

Fig. 4 *Distribution of main stress for experimental measurement on left side and for FEM simulation on right side, load 1 kN*

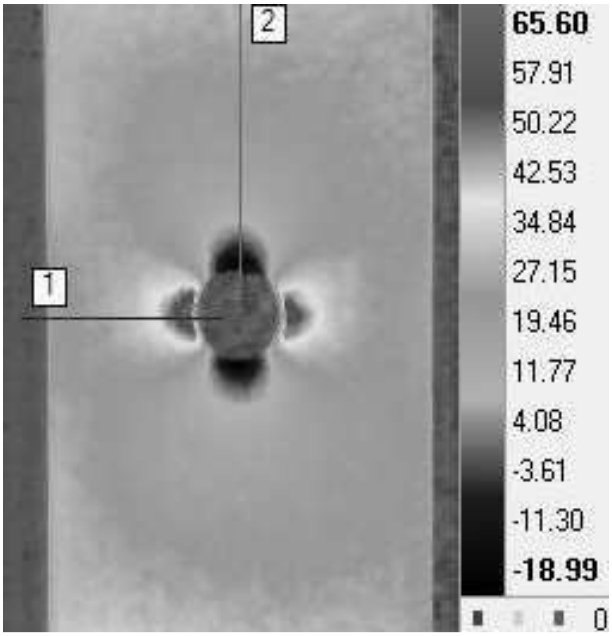

Fig. 5 *The main stresses on the Y and Z axes*

For further comparison, results were selected at the load of 1 kN, which are most appropriate due to the greatest thermal expression in the experimental part.

The distribution of main stresses in FEM simulations and experimental measurements is the same. Stress concentrators are located in the area of the circular hole. The maximum values of the main stresses are located on the sides of the hole, the minimum values are located on the top and bottom of the opening, in both cases (Fig. 4)

For a better comparison, graphs of dependence on the main stresses in MPa and positions on the specimen, respectively, on the geometric model were plotted. The areas of stress progress were selected as shown in Fig. 5. The blue curve represents the main stress trend for the experimental measurement, and the red curve represents the FEM analysis (Fig. 6,7).

On the graph of the main stress trend for a line parallel to the Y axis from the experimental measurement, we can observe a slight displacement of course of the stress. At the end, the two curves penetrate and essentially end almost at the same stress value with a few tenths of MPa difference.

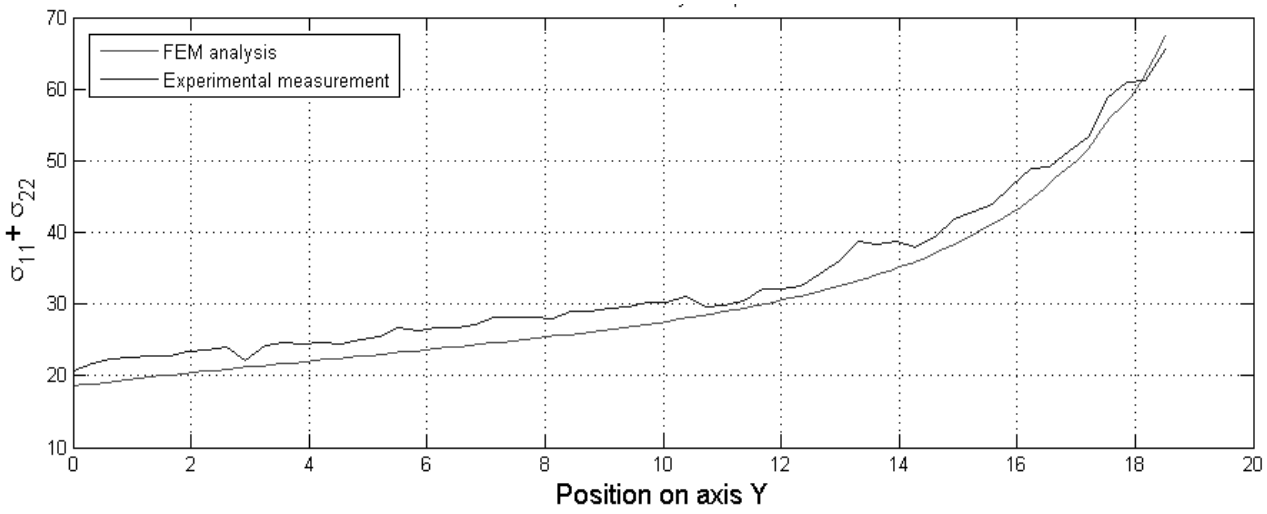

Fig. 6 *Comparison of the main stresses in the experimental measurement with the main stresses in the numerical analysis, the course by line 1*

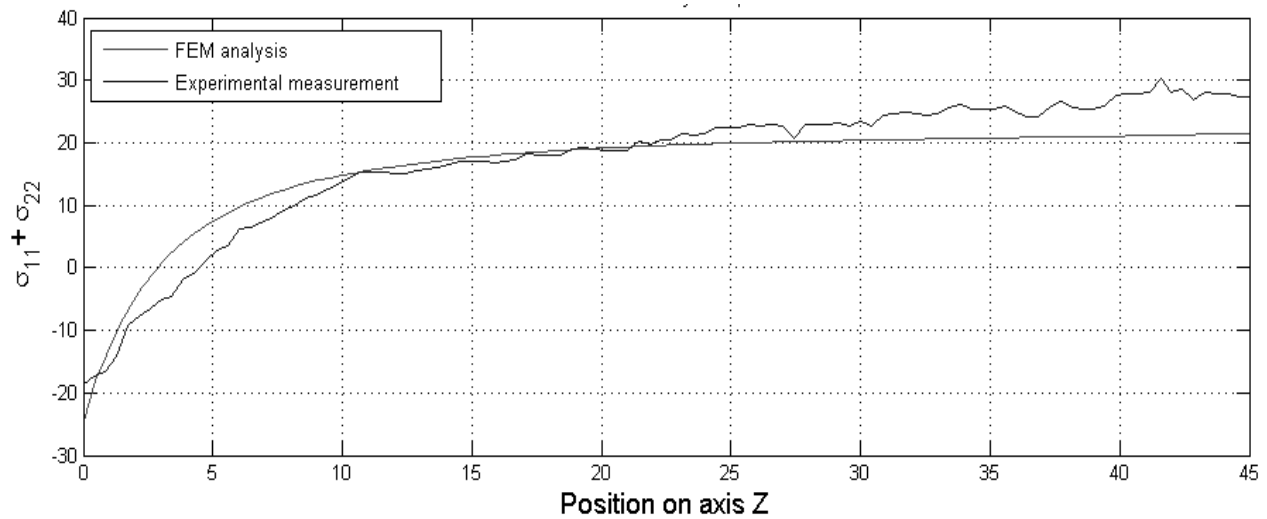

Fig. 7 *Comparison of the main stresses in the experimental measurement with the main stresses in the numerical analysis, the course by line 2*

On the plot of main stress for a line parallel to the Z axis, a slight shift between the curves at the beginning of the plot can be observed, the course being identical between 10 and 23 millimeters. From 23 millimeters, the curve moves through the experimental measurement (Fig. 7). This shift could be explained by the reflection of radiation from the environment of the jaws of the loader (Fig. 5), but we can not sufficiently prove the claim.

5 Summary

The measurement was performed on the basis of thermoelastic analysis theory. The flat specimen with hole was cyclically loaded and the evaluation was carried out after the change of the individual load levels. The stress fields of the first stress invariant were evaluated, corresponding to the sum of the main stresses. The results were compared with the numerical solution of the problem. The difference between the numerical solution and the experimental measurement was up to 4%. Based on this comparison, experimental measurement is appropriate for further use.

Acknowledgement

This article was supported by Slovak Grant Agency VEGA 13/010/00.

References

[1] VAVILOV, V. (2009). Thermal / Infrared testing. In: *Nondestructive testing*, Publishing house Spektr, 2009. – 732p.

[2] PECHAC, P., SAGA, M., (2016). Controlling of Local search Methods' Parameters in Memetic Algorithms Using the Principles of Simulated Annealing, *Procedia Engineering*, Volume 136, (2016), Pages 70-76.

[3] VASKO, M., SAGA, M. (2013). Application of fuzzy structural analysis for damage prediction considering uncertain S/N curve. *Applied Mechanics and Materials* 420 (2013), 21-29.

[4] MEOLA, C., CARLOMAGNO, G. M., RICCI F., LOPRESTO V., CAPRINO G. Investigation of Impact Damage in Composites with Infrared Thermography, *6th NDT In Progress Proceedings*, Prague (Czech Republic) P. Mazal ed., pp 175-182.

[5] XIAN, X. - ZHENG, W. - HU, W. (1986). Evaluation of the Damage of Carbon/Epoxy Composite Laminates under Static and Fatigue Loading by Thermographic Analyses.*Proceedings of the International Symposium on Composite Materials and Structures*, 710–716.

[6] ANDRIANOPOULOS, N.P., CHAMPIDIS, K.T., ILIOPOULOS, A.P. Detection of crack nucleation in sheet metal forming by monitoring infrared radiation, *Fatigue Fract Engng Mater Sruct*, №26, pp. 323-328.

[7] BANERJEE, S., RICCI, F., SHISH, F., MAL, A.K.. (2007). Health Monitoring of Composite Structures Using Ultrasonic Guided Waves. *Advanced Ultrasonic Methods for Material and Structure Inspection – Instrumentation and Measurements Series*, Edited by Tribikram Kundu, ISTE Ltd 2007; pp. 43-88.

[8] BENESOVA, S., KRIZ, A., BENES, P. (2017). Analysis of the Joint between Blade and Stator Disc in Steam Turbine. *Manufacturing Technology*, Volume 17, (2017) 3-7.

[9] BITTNER, V., TUČEK, R., PANSKÁ, Š., SVOBODA, M., JELEN K. (2017). Using the Fourier Transform in the Analysis of Vibration Load Tests of Heterogeneous Mechanical Systems. *Manufacturing Technology*, Volume 17, (2017) 839-841.

[10] WANG, Z. (2017). A Method of Computer-aided Modular Fixture Design, Part 1: Creating the Feature-model Repository of Fixture Elements. *Manufacturing Technology*, Volume 17, (2017) 110-114.

10.21062/ujep/125.2018/a/1213-2489/MT/18/3/482